UNCECOMP 2015
1st ECCOMAS Thematic Conference on
Uncertainty Quantification in Computational Sciences and Engineering
M. Papadrakakis, V. Papadopoulos, G. Stefanou (eds.)
Crete Island, Greece, 25–27 May 2015

AN INVESTIGATION OF UNCERTAINTY DUE TO STOCHASTICALLY VARYING GEOMETRY: AN INITIAL STUDY

Markus Wahlsten[1] **& Jan Nordström**[2]

[1]Department of Mathematics, Computational Mathematics, Linköping University,
SE-581 83, Linköping, Sweden
e-mail: markus.wahlsten@liu.se

[2] Department of Mathematics, Computational Mathematics, Linköping University,
SE-581 83, Linköping, Sweden,
e-mail: jan.nordstrom@liu.se

Keywords: Uncertainty Quantification, Varying Geometry, Boundary Conditions, Hyperbolic Problems

Abstract. *We study hyperbolic problems with uncertain stochastically varying geometries. Our aim is to investigate how the stochastically varying uncertainty in the geometry affects the solution of the partial differential equation in terms of the mean and variance of the solution.*

The problem considered is the two dimensional advection equation on a general domain, which is transformed using curvilinear coordinates to a unit square. The numerical solution is computed using a high order finite difference formulation on summation-by-parts form with weakly imposed boundary conditions. The statistics of the solution are computed non-intrusively using quadrature rules given by the probability density function of the random variable.

We prove that the continuous problem is strongly well-posed and that the semi-discrete problem is strongly stable. Numerical calculations using the method of manufactured solution verify the accuracy of the scheme and the statistical properties of the solution are discussed.

1 INTRODUCTION

When solving partial differential equations, uncertainty of where the boundaries of the domain are located may arise for many reasons. Examples include bad materials, imprecise manufacturing machines and non-perfect mesh generators. In this paper we study the effects of imposing the boundary condition at stochastically varying positions in space.

We start by transforming the stochastically varying domain into a fixed domain. The continuous formulation is analyzed using the energy method, and strong well-posedness is proved. The continuous problem is discretized using high order finite differences on summation-by-parts form with weakly imposed boundary conditions, and strong stability is proved. The statistics of the solution such as the mean, variance, confidence intervals are computed non-intrusively using quadrature rules for the given stochastic distributions [1, 2].

The paper will proceed as follows. In section 2 we define the continuous problem in two dimensions, transform it using curvilinear coordinates to the unit square and derive energy estimates that lead to well-posedness. Next, in section 3, we formulate a finite difference scheme for the continuous problem and prove stability. Moreover, in section 4 we compute various statistics of the problem for different stochastic settings. Finally, in section 5 we draw conclusions.

2 THE CONTINUOUS PROBLEM

Consider the advection equation in two space dimensions

$$\begin{aligned} u_t + au_x + bu_y &= F(x,y,t), \quad (x,y) \in \Omega(\theta), \quad t \geq 0 \\ Lu(x,y,t,\theta) &= g(x,y,t), \quad (x,y) \in \Gamma(\theta), \quad t \geq 0 \\ u(x,y,0,\theta) &= f(x,y), \quad (x,y) \in \Omega(\theta), \quad t = 0, \end{aligned} \tag{1}$$

where a and b are scalars, $u = (x,y,t,\theta)$ represents the solution to the problem where, θ is a random variable. $F(x,y,t)$, $g(x,y,t)$ and $f(x,y)$ are data to the problem. The goal of this study is to investigate the effects of placing the data at $(x,y) \in \Gamma(\theta)$.

2.1 Transformation

We transform the domain Ω to the unit square by introducing,

$$\begin{aligned} x = x(\xi,\eta), \quad \xi = \xi(x,y,\theta) \\ y = y(\xi,\eta), \quad \eta = \eta(x,y,\theta), \end{aligned} \tag{2}$$

where $0 \leq \xi \leq 1$ and $0 \leq \eta \leq 1$. By applying the chain rule to (1), multiplying by the Jacobian matrix J, using the metric relations and the Geometric Conservation Law (GCL), see [3], gives

$$Ju_t + [(J\xi_x a + J\xi_y b)u]_\xi + [(J\eta_x a + J\eta_y b)u]_\eta = 0. \tag{3}$$

The Jacobian matrix of the transformation given above is,

$$[J] = \begin{bmatrix} x_\xi & y_\xi \\ x_\eta & y_\eta, \end{bmatrix} \tag{4}$$

where the determinant of $[J] = J = x_\xi y_\eta - x_\eta y_\xi > 0$.

The final formulation of the transformed problem including initial and boundary conditions is

$$\begin{aligned} Ju_t + (\tilde{a}u)_\xi + (\tilde{b}u)_\eta &= 0, \quad (\xi,\eta) \in \Omega \quad t \geq 0 \\ Lu(\xi,\eta,t,\theta) &= g(\xi,\eta,t), \quad (\xi,\eta) \in \partial\Omega, \quad t \geq 0 \\ u(\xi,\eta,0,\theta) &= f(\xi,\eta), \quad (\xi,\eta) \in \Omega, \quad t = 0, \end{aligned} \tag{5}$$

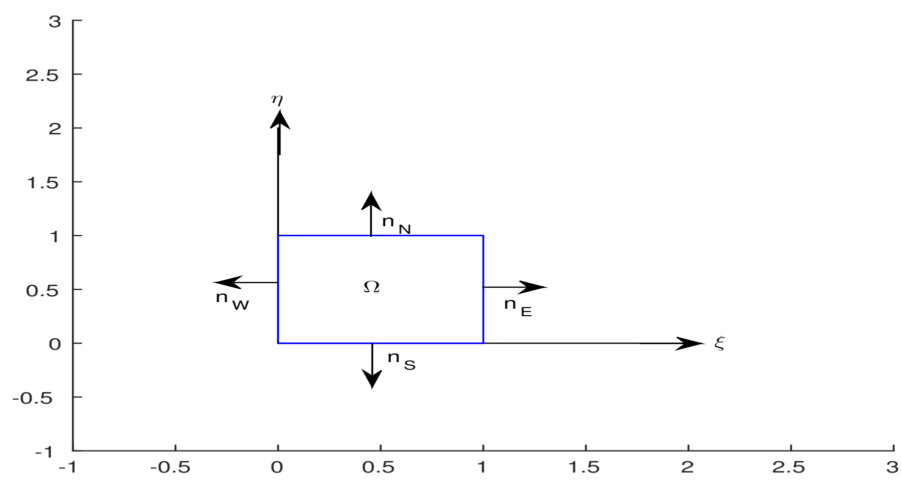

Figure 1: The transformed domain including normal vectors n_E, n_W, n_N and n_S.

where

$$\tilde{a} = y_\eta a - x_\eta b, \qquad \tilde{b} = -x_\xi a + y_\xi b, \tag{6}$$

and $\Omega = [0,1] \times [0,1]$. The transformed domain is presented in figure 1. We note that the wave speeds $\tilde{a}/J$ and $\tilde{b}/J$ depend on the stochastic variable θ.

2.2 The energy method

We multiply the transformed problem (5), with u and integrate over the domain Ω. By using (3), (6), and the Green-Gauss theorem, we obtain

$$\frac{d}{dt}\left\|u(t,\xi,\eta)\right\|_J^2 = -\oint_{\partial\Omega} u^2[(\tilde{a},\tilde{b})\cdot n]\, ds, \tag{7}$$

where n is the outward pointing normal vector. The definition $\|u\|_J^2 = \int_\Omega u^2 J\, d\xi d\eta$ has been used in (7). The right hand side (RHS) in (7) can be evaluated as

$$\frac{d}{dt}\left\|u(t,\xi,\eta)\right\|_J^2 = -\int_0^1 \tilde{a}u^2\big|_{\xi=1} - \tilde{a}u^2\big|_{\xi=0}\, d\eta - \int_0^1 \tilde{b}u^2\big|_{\eta=1} - \tilde{b}u^2\big|_{\eta=0}\, d\xi. \tag{8}$$

We note that the first boundary term in (8) can be rewritten as

$$\begin{aligned} \int_0^1 \tilde{a}u^2\big|_{\xi=1}\, d\eta &= \int_0^1 u^2\big|_{\xi=1}(a,b)\cdot(y_\eta,-x_\eta)\, d\eta \\ &= \int_0^1 u^2\big|_{\xi=1}(a,b)\cdot\tfrac{(y_\eta,-x_\eta)}{\sqrt{y_\eta^2+x_\eta^2}}\sqrt{y_\eta^2+x_\eta^2}\, d\eta \\ &= \oint_{\delta\Omega} u^2\big|_{\xi=1}(a,b)\cdot n_E\, ds_\eta, \end{aligned} \tag{9}$$

where $ds = ds_\eta = \sqrt{y_\eta^2 + x_\eta^2}\, d\eta$ since ξ is constant. Further, the outward pointing normal vector at this boundary is denoted $n_E = \frac{(y_\eta,-x_\eta)}{\sqrt{y_\eta^2+x_\eta^2}}$ where E denotes the east boundary, see Figure 1. By using similar arguments for the remaining boundaries, we obtain

$$\begin{aligned} \tfrac{d}{dt}\left\|u(t,\xi,\eta)\right\|_J^2 = &- \oint u^2\big|_{\xi=1}(a,b)\cdot n_E + u^2\big|_{\xi=0}(a,b)\cdot n_W\, ds_\eta \\ &- \oint u^2\big|_{\eta=1}(a,b)\cdot n_N + u^2\big|_{\eta=0}(a,b)\cdot n_S\, ds_\xi. \end{aligned} \tag{10}$$

To bound the energy, we impose boundary conditions when $(a,b)\cdot n_{E,W,N,S} < 0$, see Figure 1. Due to the fact that a and b can vary, we can, using the indicator function $\mathbf{1}$, impose boundary data in the following general way,

$$\begin{aligned}
\tfrac{d}{dt}\|u(t,\xi,\eta)\|_J^2 = &- \oint (a,b)\cdot n_E \mathbf{1}_+((a,b)\cdot n_E)(u^2\big|_{\xi=1} - g(0,\eta,t)^2)\,ds \\
&- \oint (a,b)\cdot n_E \mathbf{1}_+((a,b)\cdot n_E)(u^2\big|_{\xi=0} - g(1,\eta,t)^2)\,ds \\
&- \oint (a,b)\cdot n_N \mathbf{1}_+((a,b)\cdot n_N)(u^2\big|_{\eta=1} - g(\xi,1,t)^2)\,ds \\
&- \oint (a,b)\cdot n_N \mathbf{1}_+((a,b)\cdot n_N)(u^2\big|_{\eta=0} - g(\xi,0,t)^2)\,ds,
\end{aligned} \tag{11}$$

where

$$\mathbf{1}_+(M) = \begin{cases} 1 & \text{if } M > 0 \\ 0 & \text{else} \end{cases} \qquad \mathbf{1}_-(M) = \begin{cases} 1 & \text{if } M < 0 \\ 0 & \text{else ,} \end{cases} \tag{12}$$

In (11), to ease the notation, n_W and n_S are replaced by $-n_E$ and $-n_N$ respectively.

We can now prove

Proposition 1. *The problem (5) with non-homogeneous boundary conditions is strongly stable.*

Proof. Time integration of (11) in time results in

$$\begin{aligned}
\|u(T,\xi,\eta)\|_J^2 = &- \int_0^T \oint (a,b)\cdot n_E \mathbf{1}_+((a,b)\cdot n_E)(u^2\big|_{\xi=1} - g(0,\eta,t)^2)\,dsdt \\
&- \int_0^T \oint (a,b)\cdot n_W \mathbf{1}_+((a,b)\cdot n_W)(u^2\big|_{\xi=0} - g(1,\eta,t)^2)\,dsdt \\
&- \int_0^T \oint (a,b)\cdot n_N \mathbf{1}_+((a,b)\cdot n_N)(u^2\big|_{\eta=1} - g(\xi,1,t)^2)\,dsdt \\
&- \int_0^T \oint (a,b)\cdot n_S \mathbf{1}_+((a,b)\cdot n_S)(u^2\big|_{\eta=0} - g(\xi,0,t)^2)\,dsdt \\
&+ \|f\|_J^2\,.
\end{aligned} \tag{13}$$

In (13), the boundary terms without data give a non-positive contribution, hence the solution is bounded by data and strongly stable. □

3 THE NUMERICAL SCHEME

In this section we consider the numerical approximation of (5) formulated using the summation-by-parts operators with simultaneous approximation terms (SBP-SAT) technique. First, we rewrite our transformed continuous problem (5) using the splitting technique described in [4], to obtain,

$$Ju_t + \tfrac{1}{2}[(\tilde{a}u)_\xi + \tilde{a}u_\xi + \tilde{a}_\xi u] + \tfrac{1}{2}[(\tilde{b}u)_\eta + \tilde{b}u_\eta + \tilde{b}_\eta u] = 0. \tag{14}$$

The corresponding semi-discrete version of (14) including penalty terms for the boundary conditions is

$$\begin{aligned}
\tilde{J}U_t &+ \tfrac{1}{2}[(P_\xi^{-1}Q_\xi \otimes I_\eta)\tilde{A}U + \tilde{A}(P_\xi^{-1}Q_\xi \otimes I_\eta)U + \tilde{A}_\xi U] \\
&+ \tfrac{1}{2}[(I_\xi \otimes P_\eta^{-1}Q_\eta)\tilde{B}U + \tilde{B}(I_\xi \otimes P_\eta^{-1}Q_\eta)U + \tilde{B}_\eta U] \\
&= \sigma_1(P_\xi^{-1}E_{0N} \otimes I_\eta)(U - (E_{0N} \otimes I_\eta)g) \\
&+ \sigma_2(P_\xi^{-1}E_{NN} \otimes I_\eta)(U - (E_{NN} \otimes I_\eta)g) \\
&+ \sigma_3(I_\xi \otimes P_\eta^{-1}E_{0M})(U - (I_\xi \otimes E_{0M})g) \\
&+ \sigma_4(I_\xi \otimes P_\eta^{-1}E_{MM})(U - (I_\xi \otimes E_{MM})g) \\
U(0) &= f.
\end{aligned} \tag{15}$$

In (15), $P^{-1}Q$ is the finite difference operator, P is a positive definite matrix, Q is an almost skew-symmetric matrix satisfying $Q + Q^T = B = diag[-1,0,\ldots,0,1]$. E_{0N} and E_{0M} are zero matrices with the exception of the first element which is equal to one, the corresponding sizes of the matrices are $N+1 \times N+1$ and $M+1 \times M+1$. The notations I_ξ, I_η corresponds to the identity matrices of sizes $N+1 \times N+1$, $M+1 \times M+1$. $\tilde{A}$, $\tilde{B}$ and $\tilde{J}$ are diagonal matrices approximating $\tilde{a}$, $\tilde{b}$ and J point wise. $\sigma_1, \sigma_2, \sigma_3$ and σ_4 are chosen such that the numerical scheme (15) is stable. U is a vector containing the numerical solution where, $U_{i,j}$ approximates $u(\xi_i, \eta_j)$ ordered as,

$$U = \begin{bmatrix} U_0 \\ U_1 \\ \vdots \\ U_N \end{bmatrix}, \qquad U_i = \begin{bmatrix} U_{i,0} \\ U_{i,1} \\ \vdots \\ U_{i,M} \end{bmatrix}, \tag{16}$$

where $i = 0, 1, \ldots, N$ corresponds to the grid points in ξ and $i = 0, 1, \ldots, M$ to the grid points in η. For more details on the SBP-SAT techniques, see [5].

For stability, the following lemma is required.

Lemma 1. *The Numerical Geometric Conservation Law (NGCL):*

$$\tilde{A}_\xi + \tilde{B}_\eta = 0, \tag{17}$$

holds.

Proof. The matrices $\tilde{A}_\xi$ and $\tilde{B}_\eta$ approximating $\tilde{a}_\xi$ and $\tilde{b}_\eta$ are defined in the following way

$$\tilde{A}_\xi = (\tilde{y_\eta})_\xi a - (\tilde{x_\eta})_\xi b, \qquad \tilde{B}_\eta = -(\tilde{y_\xi})_\eta a + (\tilde{x_\xi})_\eta b, \tag{18}$$

where the matrices $(\tilde{y_\eta})_\xi$, $(\tilde{x_\eta})_\xi$, $(\tilde{y_\xi})_\eta$ and $(\tilde{x_\xi})_\eta$ approximates $(y_\eta)_\xi$, $(x_\eta)_\xi$, $(y_\xi)_\eta$ and $(x_\xi)_\eta$ point wise respectively. The matrices are defined as

$$\begin{array}{lllllll} (\tilde{y_\eta})_\xi & = & diag[D_\xi(D_\eta y)], & (\tilde{x_\eta})_\xi & = & diag[D_\xi(D_\eta x)], \\ (\tilde{y_\xi})_\eta & = & diag[D_\eta(D_\xi y)], & (\tilde{x_\xi})_\eta & = & diag[D_\eta(D_\xi x)]. \end{array} \tag{19}$$

In (19), D_ξ and D_η denotes finite difference operators of the form $D_\xi = (P_\xi^{-1}Q_\xi \otimes I_\eta)$ and $D_\eta = (I_\xi \otimes P_\eta^{-1}Q_\eta)$ respectively. x and y are discrete Cartesian coordinates in the domain Ω.

Next, by using the definitions (18) and (19) in (17) we obtain,

$$\tilde{A}_\xi + \tilde{B}_\eta = a[D_\xi(D_\eta y) - D_\eta(D_\xi y)] + b[-D_\xi(D_\eta x) + D_\eta(D_\xi x)]. \tag{20}$$

The RHS of (20) is zero if the differential operators commute, that is $D_\xi D_\eta = D_\eta D_\xi$. This property follows directly from the properties of the Kronecker product, since

$$\begin{array}{lll} D_\xi D_\eta & = & (P_\xi^{-1}Q_\xi \otimes I_\eta)(I_\xi \otimes P_\eta^{-1}Q_\eta) = (P_\xi^{-1}Q_\xi \otimes P_\eta^{-1}Q_\eta) \\ & = & (I_\xi \otimes P_\eta^{-1}Q_\eta)(P_\xi^{-1}Q_\xi \otimes I_\eta) = D_\eta D_\xi. \end{array} \tag{21}$$

The use of (21) in (20) proves the lemma. □

3.1 Stability

To prove stability we multiply (15) from the left with $U^T(P_\xi \otimes P_\eta)$, add the transpose and define the discrete norm $\|U\|^2_{J(P_\xi \otimes P_\eta)} = U^T \tilde{J}(P_\xi \otimes P_\eta)U$ to obtain

$$
\begin{aligned}
\tfrac{d}{dt}\|U\|^2_{J(P_\xi\otimes P_\eta)} &+ \tfrac{1}{2}[U^T(Q_\xi + Q_\xi^T \otimes P_\eta)\tilde{A}U + \tilde{A}U^T(Q_\xi + Q_\xi^T \otimes P_\eta)U] \\
&+ \tfrac{1}{2}[U^T(P_\xi \otimes Q_\eta + Q_\eta^T)\tilde{B}U + \tilde{B}U^T(P_\xi \otimes Q_\eta + Q_\eta^T)U] \\
&+ \tilde{A}_\xi U^T(P_\xi \otimes P_\eta)U + \tilde{B}_\eta U^T(P_\xi \otimes P_\eta)U \\
&= \sigma_1 U^T(E_{0N} \otimes P_\eta)(U - (E_{0N} \otimes I_\eta)g) \\
&+ \sigma_2 U^T(E_{NN} \otimes P_\eta)(U - (E_{NN} \otimes I_\eta)g) \\
&+ \sigma_3 U^T(P_\xi \otimes E_{0M})(U - (I_\xi \otimes E_{0M})g) \\
&+ \sigma_4 U^T(P_\xi \otimes E_{MM})(U - (I_\xi \otimes E_{MM})g).
\end{aligned}
\tag{22}
$$

By observing that $Q_\xi + Q_\xi^T = E_{NN} - E_{0N}$, $Q_\eta + Q_\eta^T = E_{MM} - E_{0M}$ and using the notation $\tilde{g}_1 = (E_{0N} \otimes I_\eta)g$, $\tilde{g}_2 = (E_{NN} \otimes I_\eta)g$, $\tilde{g}_3 = (I_\xi \otimes E_{0M})g$, $\tilde{g}_4 = (I_\xi \otimes E_{MM})g$ and $I_{\xi\eta} = (I_\xi \otimes I_\eta)$ we can rewrite (22) as

$$
\begin{aligned}
\tfrac{d}{dt}\|U\|^2_{J(P_\xi\otimes P_\eta)} &= (\tilde{A} + 2\sigma_1 I_{\xi\eta})U^T(E_{0N} \otimes P_\eta)U \\
&- (\tilde{A} - 2\sigma_2 I_{\xi\eta})U^T(E_{NN} \otimes P_\eta)U \\
&+ (\tilde{B} + 2\sigma_3 I_{\xi\eta})U^T(P_\xi \otimes E_{0M})U \\
&- (\tilde{B} - 2\sigma_4 I_{\xi\eta})U^T(P_\xi \otimes E_{MM})U \\
&- 2\sigma_1 U^T(E_{0N} \otimes P_\eta)\tilde{g}_1 - 2\sigma_2 U^T(E_{NN} \otimes P_\eta)\tilde{g}_2 \\
&- 2\sigma_3 U^T(P_\eta \otimes E_{0M})\tilde{g}_3 - 2\sigma_4 U^T(P_\eta \otimes E_{MM})\tilde{g}_4 \\
&- U^T(\tilde{a}_\xi + \tilde{b}_\eta)(P_\xi \otimes P_\eta)U.
\end{aligned}
\tag{23}
$$

By adding and subtracting the terms

$$
\begin{aligned}
&\sigma_1^2(\tilde{A} + 2\sigma_1 I_{\xi\eta})^{-1}\tilde{g}_1^T(E_{0N} \otimes P_\eta)\tilde{g}_1, \quad \sigma_2^2(\tilde{A} - 2\sigma_2 I_{\xi\eta})^{-1}\tilde{g}_2^T(E_{NN} \otimes P_\eta)\tilde{g}_2, \\
&\sigma_3^2(\tilde{B} + 2\sigma_3 I_{\xi\eta})^{-1}\tilde{g}_3^T(P_\xi \otimes E_{0M})\tilde{g}_3, \quad \sigma_4^2(\tilde{B} - 2\sigma_4 I_{\xi\eta})^{-1}\tilde{g}_4^T(P_\xi \otimes E_{MM})\tilde{g}_4,
\end{aligned}
$$

in (23) gives

$$
\begin{aligned}
\tfrac{d}{dt}\|U\|^2_{J(P_\xi\otimes P_\eta)} &= \sigma_1^2(\tilde{A} + 2\sigma_1 I_{\xi\eta})^{-1}\tilde{g}_1^T(E_{0N} \otimes P_\eta)\tilde{g}_1 \\
&- \sigma_2^2(\tilde{A} - 2\sigma_2 I_{\xi\eta})^{-1}\tilde{g}_2^T(E_{NN} \otimes P_\eta)\tilde{g}_2 \\
&+ \sigma_3^2(\tilde{B} + 2\sigma_3 I_{\xi\eta})^{-1}\tilde{g}_3^T(P_\xi \otimes E_{0M})\tilde{g}_3 \\
&- \sigma_4^2(\tilde{B} - 2\sigma_4 I_{\xi\eta})^{-1}\tilde{g}_4^T(P_\xi \otimes E_{MM})\tilde{g}_4 \\
&+ (\tilde{A} + 2\sigma_1 I_{\xi\eta})(U - \sigma_1(\tilde{A} + 2\sigma_1 I_{\xi\eta})^{-1}\tilde{g}_1)^T \\
&\quad (E_{0N} \otimes P_\eta)(U - \sigma_1(\tilde{A} + 2\sigma_1 I_{\xi\eta})^{-1}\tilde{g}_1) \\
&- (\tilde{A} - 2\sigma_2 I_{\xi\eta})(U - \sigma_2(\tilde{A} - 2\sigma_2 I_{\xi\eta})^{-1}\tilde{g}_2)^T \\
&\quad (E_{NN} \otimes P_\eta)(U - \sigma_2(\tilde{A} - 2\sigma_2 I_{\xi\eta})^{-1}\tilde{g}_2) \\
&+ (\tilde{B} + 2\sigma_3 I_{\xi\eta})(U - \sigma_3(\tilde{B} + 2\sigma_3 I_{\xi\eta})^{-1}\tilde{g}_3)^T \\
&\quad (P_\xi \otimes E_{0M})(U - \sigma_3(\tilde{B} + 2\sigma_3 I_{\xi\eta})^{-1}\tilde{g}_3) \\
&- (\tilde{B} - 2\sigma_4 I_{\xi\eta})(U - \sigma_4(\tilde{B} - 2\sigma_4 I_{\xi\eta})^{-1}\tilde{g}_4)^T \\
&\quad (P_\xi \otimes E_{MM})(U - \sigma_4(\tilde{B} - 2\sigma_4 I_{\xi\eta})^{-1}\tilde{g}_4).
\end{aligned}
\tag{24}
$$

To mimic the continuous estimate (11), the following choices of penalty parameters are made,

$$
\sigma_1 = -\tfrac{\tilde{a}+|\tilde{a}|}{2}, \qquad \sigma_2 = \tfrac{\tilde{a}-|\tilde{a}|}{2}, \qquad \sigma_3 = -\tfrac{\tilde{b}+|\tilde{b}|}{2}, \qquad \sigma_4 = \tfrac{\tilde{b}-|\tilde{b}|}{2}. \tag{25}
$$

Note again that we obtain stochastically varying penalty parameters.

By using the penalty parameters (25) in (24) we obtain

$$\begin{array}{rcl} \frac{d}{dt}\|U\|^2_{J(P_\xi\otimes P_\eta)} & = & \tilde{A}\mathbf{1}_+(\tilde{A})(\tilde{g}_1^T(E_{0N}\otimes P_\eta)\tilde{g}_1 - U^T(E_{NN}\otimes P_\eta)U) \\ & - & \tilde{A}\mathbf{1}_-(\tilde{A})(\tilde{g}_2^T(E_{NN}\otimes P_\eta)\tilde{g}_2 - U^T(E_{0N}\otimes P_\eta)U) \\ & + & \tilde{B}\mathbf{1}_+(\tilde{B})(\tilde{g}_3^T(P_\xi\otimes E_{0M})\tilde{g}_3 - U^T(P_\xi\otimes E_{MM})U) \\ & - & \tilde{B}\mathbf{1}_-(\tilde{B})(\tilde{g}_4^T(P_\xi\otimes E_{MM})\tilde{g}_4 - U^T(P_\xi\otimes E_{0M})U) \\ & - & \tilde{A}\mathbf{1}_+(\tilde{A})(U-\tilde{g}_1)^T(E_{0N}\otimes P_\eta)(U-\tilde{g}_1) \\ & + & \tilde{A}\mathbf{1}_-(\tilde{A})(U-\tilde{g}_2)^T(E_{NN}\otimes P_\eta)(U-\tilde{g}_2) \\ & - & \tilde{B}\mathbf{1}_+(\tilde{B})(U-\tilde{g}_3)^T(P_\xi\otimes E_{0M})(U-\tilde{g}_3) \\ & + & \tilde{B}\mathbf{1}_-(\tilde{B})(U-\tilde{g}_4)^T(P_\xi\otimes E_{MM})(U-\tilde{g}_4), \end{array} \tag{26}$$

where $\mathbf{1}$ denotes the indicator function defined above. By (26) we obtain a discrete estimate.

We can now prove

Proposition 2. *The numerical approximation (15) using the penalty coefficients*

$$\sigma_1 = -\frac{\tilde{a}+|\tilde{a}|}{2}, \qquad \sigma_2 = \frac{\tilde{a}-|\tilde{a}|}{2}, \qquad \sigma_3 = -\frac{\tilde{b}+|\tilde{b}|}{2}, \qquad \sigma_4 = \frac{\tilde{b}-|\tilde{b}|}{2}, \tag{27}$$

is strongly stable.

Proof. By integrating (26) in time using the penalty parameters in (27) leads to

$$\begin{array}{rcl} \|U\|^2_{J(P_\xi\otimes P_\eta)} & = & \int_0^T \tilde{A}\mathbf{1}_+(\tilde{A})(\tilde{g}_1^T(E_{0N}\otimes P_\eta)\tilde{g}_1 - U^T(E_{NN}\otimes P_\eta)U)dt \\ & - & \int_0^T \tilde{A}\mathbf{1}_-(\tilde{A})(\tilde{g}_2^T(E_{NN}\otimes P_\eta)\tilde{g}_2 - U^T(E_{0N}\otimes P_\eta)U)dt \\ & + & \int_0^T \tilde{B}\mathbf{1}_+(\tilde{B})(\tilde{g}_3^T(P_\xi\otimes E_{0M})\tilde{g}_3 - U^T(P_\xi\otimes E_{MM})U)dt \\ & - & \int_0^T \tilde{B}\mathbf{1}_-(\tilde{B})(\tilde{g}_4^T(P_\xi\otimes E_{MM})\tilde{g}_4 - U^T(P_\xi\otimes E_{0M})U)dt \\ & - & \int_0^T \tilde{A}\mathbf{1}_+(\tilde{A})(U-\tilde{g}_1)^T(E_{0N}\otimes P_\eta)(U-\tilde{g}_1)dt \\ & + & \int_0^T \tilde{A}\mathbf{1}_-(\tilde{A})(U-\tilde{g}_2)^T(E_{NN}\otimes P_\eta)(U-\tilde{g}_2)dt \\ & - & \int_0^T \tilde{B}\mathbf{1}_+(\tilde{B})(U-\tilde{g}_3)^T(P_\xi\otimes E_{0M})(U-\tilde{g}_3)dt \\ & + & \int_0^T \tilde{B}\mathbf{1}_-(\tilde{B})(U-\tilde{g}_4)^T(P_\xi\otimes E_{MM})(U-\tilde{g}_4)dt \\ & + & \|f\|^2_{J(P_\xi\otimes P_\eta)}. \end{array} \tag{28}$$

As in the continuous energy estimate, the negative boundary terms not involving data in (28) results in a strongly stable numerical approximation. □

Remark 1. *Note the resemblence between the discrete energy estimate (26) and its continuous counterpart (11).*

4 NUMERICAL AND STATISTICAL RESULTS

In this section we will compute various statistics for the given model problem (1) using the parameters $a = b = -1$. We use the method of manufactured solution [6] to compute the accuracy of the scheme.

4.1 Rate of convergence

The rate of convergence is verified by computing the order of accuracy p defined as,

$$p = \log_2\left(\frac{\|e_h\|_P}{\left\|e_{\frac{h}{2}}\right\|_P}\right), \qquad \|e_h\| = \|u_a - u_h\|. \tag{29}$$

SBP operator	$N_x = Ny = 15$	$N_x = Ny = 20$	$N_x = Ny = 25$
2nd order	1.318	1.669	1.818
3rd order	2.831	3.025	3.074

Table 1: The order of accuracy for the 2nd and 3rd order SBP-SAT schemes for different number of grid points in space.

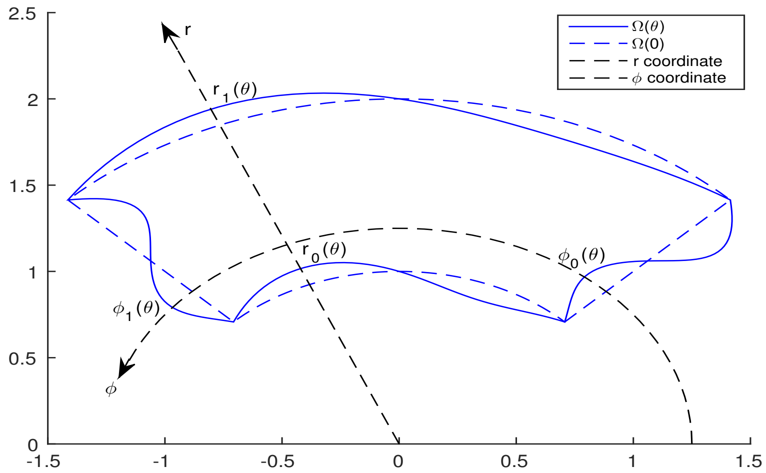

Figure 2: A schematic of the computational domain in a polar coordinate system including definitions of r_0, r_1, ϕ_0 and ϕ_1.

In (29), e_h and u_h are the error and numerical solution using the grid spacing h. The corresponding manufactured analytical solution is denoted u_a. The order of accuracy computed for different number of grid points and SBP-operators is shown in Table 1.

In the calculations below, the 3rd order SBP-operators are used on a grid with 40 grid points in both space directions and 1000 grid points in time.

4.1.1 Normally distributed stochastic data

As in the previous section we assume a normally distributed stochastic variable $\theta \sim N(0, 1)$. The stochastic dependence is enforced on the boundaries as

$$\begin{aligned} r_0(\theta) &= 1 - 0.05\theta \sin(4\phi - \pi), \\ r_1(\theta) &= 2 - 0.05\theta \sin(4\phi - \pi), \\ \phi_0(\theta) &= \tfrac{\pi}{4} + 0.05\theta \sin(2\pi(r - 1)), \\ \phi_1(\theta) &= \tfrac{3\pi}{4} + 0.05\theta \sin(2\pi(r - 1)) \end{aligned} \tag{30}$$

The quantities r_0, r_1, ϕ_0 and ϕ_1 with the computational domain are depicted in figure (2). The boundary and initial data are chosen as,

$$\begin{aligned} g(x, y, t) &= \sin(2\pi(x - t)) + \sin(2\pi(y - t)), \\ f(x, y) &= \sin(2\pi x) + \sin(2\pi y). \end{aligned} \tag{31}$$

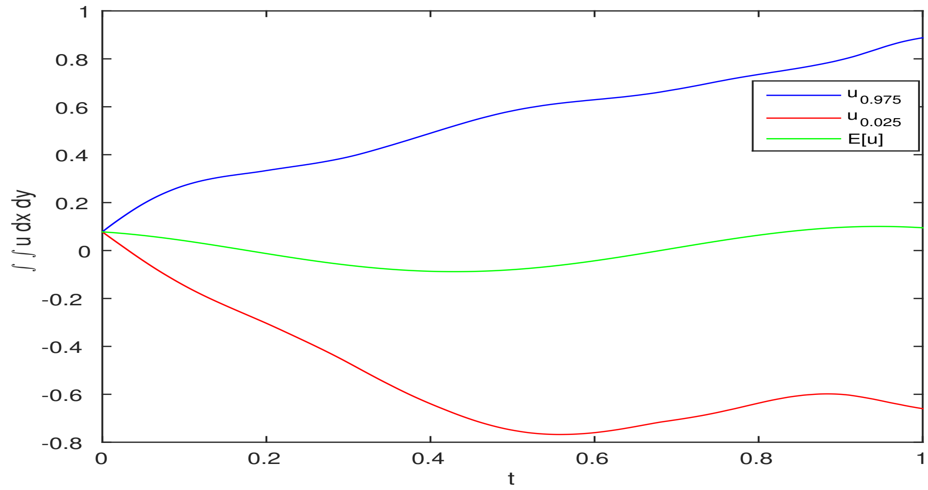

Figure 3: The mean and 95% confidence interval of the integral of the solution.

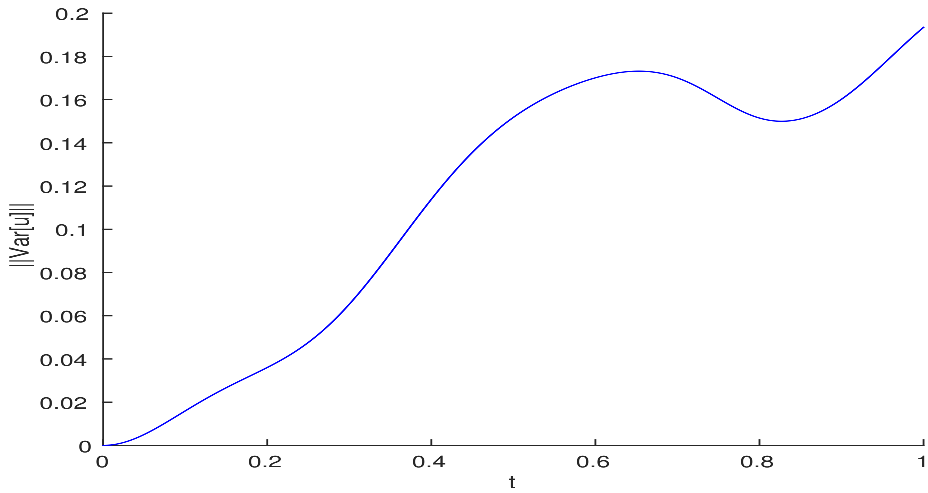

Figure 4: The L_1-norm of the variance of the solution.

In Figure 3, the mean and 95% confidence interval of the integral of the solution as a function of time is illustrated. The integral of the solution is given by

$$\iint_{\Omega} u(x, y, t, \theta)\, dxdy. \tag{32}$$

The L_1-norm of the variance of the solution is depicted in Figure 4. As can be seen, both the confidence interval and the variance grows with time.

5 CONCLUSIONS

We have studied how the solution to a partial differential equation is affected by imposing boundary data on a stochastically varying geometry. The problem was transformed to the unit square resulting in a partial differential equation with stochastically varying wave speeds. Strong well-posedness and strong stability was proven. It was shown that the stochastically varying domain lead to a numerical scheme with stochastically varying penalty parameters.

Next, the model problem was studied numerically with a small normally distributed stochastically varying geometry. It was shown that the correct convergence rates were obtained. The mean, variance and confidence intervals were computed. It was shown that the variance in the solution as well as the confidence level grows in time.

The numerical results regarding the variance and confidence intervals show that a stochastically varying geometry description affect the solution in a non-negligible way. To conclude what effects the choice of random distribution has on the solution, further investigation is needed.

Acknowledgements

The UMRIDA project has received funding from the European Union's Seventh Framework Programme for research, technological development and demonstration under grant agreement No. ACP3-GA-2013-605036.

REFERENCES

[1] G. Lin, A.M. Tartakovsky, and D.M. Tartakovsky, Uncertainty quantification via random domain decomposition and probabilistic collocation on sparse grids *Journal of Computational Physics*, **229**, 6995–7012, 2010.

[2] M.A.A. Mendes, S. Rayb, J.M.C. Pereira, J.C.F. Pereira, and D. Trimis, Quantification of uncertainty propagation due to input parameters for simple heat transfer problems *International Journal of Thermal Sciences*, **60**, 94–105, 2012.

[3] C. Farhat, P. Geuzaine, and C. Grandmont, The discrete geometric conservation law and the nonlinear stability of ALE schemes for the solution of flow problems on moving grids *Journal of Computational Physics*, **174**, 669–694, 2001.

[4] J. Nordström, Conservative Finite Difference Formulations, Variable Coefficients, Energy Estimates and Artificial Dissipation *Journal of Scientific Computing*, **29**, 375–404, 2006.

[5] M. Svärd, and J. Nordström, Review of summation-by-parts schemes for initial-boundary-value problems *Journal of Computational Physics*, **268**, 17–38, 2014.

[6] J. Nordström, and M. Wahlsten Variance reduction through robust design of boundary conditions for stochastic hyperbolic systems of equations, *Journal of Computational Physics*, **282**, 1–22, 2015.